IEICE TRANS. COMMUN., VOL.E93–B, NO.11 NOVEMBER 2010

PAPER Special Section on Fundamental Issues on Deployment of Ubiquitous Sensor Networks

A 4.78 μs Dynamic Compensated Inductive Coupling Transceiver for Ubiquitous and Wearable Body Sensor Network*

Seulki LEE[†a)], ***Student Member***, **Jerald YOO**[††], ***and*** **Hoi-Jun YOO**[†], ***Nonmembers***

SUMMARY A Real-time Capacitor Compensation (RCC) scheme is proposed for low power and continuous communication in the wearable inductive coupling transceiver. Since inductance values of wearable inductor vary dynamically with deterioration of its communication characteristics, the inductance value is monitored and its resonance frequency is adjusted by additive parallel/serial capacitors in real time. RLC Bridge for detection of the inductance variations and the Dual-edge Sampling Comparator for recognition of the variance direction are proposed. It is implemented in a 0.18 μm CMOS technology, and it occupies a $1 \times 2.7\,\mathrm{mm}^2$ chip area. The proposed transceiver consumes only 426.6 μW at 4 Mbps data rate. The compensation time takes 4.78 μs, including 3 μs of detection and 1.78 μs for compensation process in worst case.

key words: *inductive coupling, low power transceiver, short range wireless communication, wearable body sensor network, ubiquitous sensor network*

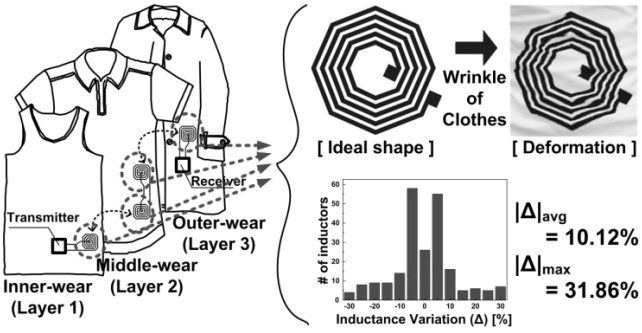

Fig. 1 System concept and inductor deformation (Measurement).

1. Introduction

Recently, wearable solutions receive more and more attention for the daily healthcare applications [1]. People want to check their health status at anytime anywhere wearing plain clothes without bothering their daily life activities. For the enhanced wearability by using the daily clothes, wearable solutions based on the fabric substrates have been proposed [2], [3]. Wireless sensor network, which integrates wireless communication with sensors, is usually exploited in the wearable healthcare system. Especially in wearable applications of less than 1 cm distance, inductive coupling or electromagnetic induction based on the wearable inductors on fabric substrates is very versatile [3]–[7]. However, in this case, the clothes or shapes of the fabric substrates can be easily deformed due to its enhanced flexibility and active motion of the wearers even though they are suitable for wearability. When the communication channel or antenna is implemented on the fabric substrate, its shape is highly susceptible to deformation. Therefore, it is crucial to minimize its effect on the communication characteristics.

Figure 1 shows the concept of the system for wearable body sensor network where the wearable inductors are placed in each layer of clothes, which is previously proposed in [5]. A pair of inductor located on the corresponding places of each layer is used for inter-layer communication. And the wireline network made of conductive yarn is installed for intra-layer communication. This system consumes lower energy compared to the conventional RF communication, and assures higher wearability compared to the conventional only wireline networks for inter-layer communication [8]. However, the wearable inductor fabrication technology on the fabric substrate is not so precision technology as the semiconductor process. Moreover, there is the dynamic variation which occurs when the user is moving with the clothes on due to the warp of the fabric substrates as shown in Fig. 1. According to the measured values of the wearable inductor in Fig. 1, the dynamic variances are up to 31.86% (10.12% in average). These large variations make the wearable inductive coupling communication very unreliable, and that's why it has not been widely used so far in inter-layer communication for wearable healthcare system in spite of its advantage in power dissipation and wearability. Although the static compensation for both variances is achieved in [5], it cannot support the dynamic compensation in real-time so that data is continuously missed until the compensation is started.

In this paper, we propose a wearable inductive coupling transceiver with dynamic compensation of inductance variations for robust communication. Especially, Real-time Capacitor Compensation (RCC) scheme is proposed with binary-weighted capacitor banks with 500 fF unit capacitance for quick compensation. Using this scheme, we can achieve low power consumption, high wearability and reliable communication at the same time. From the next sec-

Manuscript received March 2, 2010.
Manuscript revised June 21, 2010.

[†]The authors are with the Korea Advanced Institute of Science and Technology (KAIST), Daejeon, Korea.
[††]The author is with Microsystems Engineering, Marsdar Institute, Abu Dhabi, United Arab Emirates, and also with Microsystems Technology Laboratory, Massachusetts Institute of Technology, Cambridge.

*This work is supported by the Midcareer Researcher Program through the National Research Foundation of Korea (NRF) under Grant 2009-0086631 funded by the Korean government (MEST).

a) E-mail: sklee@eeinfo.kaist.ac.kr

DOI: 10.1587/transcom.E93.B.2892

tion, the detail design will be explained. In Sect. 2, the proposed wearable inductor and inductor channel design will be discussed. Section 3 describes the proposed transceiver design, and Sect. 4 explains the proposed Real-time Capacitor Compensation (RCC) scheme. And then the implementation results will be shown in Sect. 5. Finally, conclusions will be made in Sect. 6.

2. Wearable Inductor Channel Design

2.1 Wearable Inductor

The wearable inductor means the inductor formed on the fabric substrate. There are two types of wearable inductors. One is the woven inductor made by stitching conductive yarn [8] in the spiral embroidery, and the other is the planar inductor by screen printing conductive ink on the fabric [9]. In this work, only the latter type of wearable inductor is considered as shown in Fig. 2. This technology of screen printing conductive ink on the fabric is called Planar Fashionable Circuit Board (P-FCB) [9], [10], and it is also shown that it can implement the wireline network on the clothes quickly with low cost [3]. Since these inductor are formed on the fabric substrate, i.e. clothes, they should maintain their performance after washing or laundry. The inductor characteristic as an antenna is highly related with its resistance, the resistance measurement over the number of washing is performed and analyzed [9], [10]. As a result, it is shown that the resistance is not increased over 10% up to 20 times of washing even for non-covered case. And the durability to washing is enhanced if the line is covered with other materials. Therefore, the planar wearable inductor can maintain high efficiency after washing process.

In the planar wearable inductor, there are 3 parameters to determine the inductance value, the number of turns (n), average diameter (d), and the line spacing (s) as shown in Fig. 2(b). Although the inductance also has the relationship with the line width (w) parameter in planar type of inductor [12], w is not considered in this work to make the condition simple. The following relationships between the parameters and the inductance value (L) can be obtained:

$$L \propto \frac{n \cdot d}{s} \tag{1}$$

where the inductance is proportional to the number of turns and the average diameter, but inversely proportional to the line spacing. Among these parameters, the average diameter and the line spacing have the most effect on the inductance variation during manufacturing process. For example, the printed conductive ink can be spread wide over the target value to decrease the line spacing or slightly increase the average diameter. It is shown that static variation amounts to 17% [6].

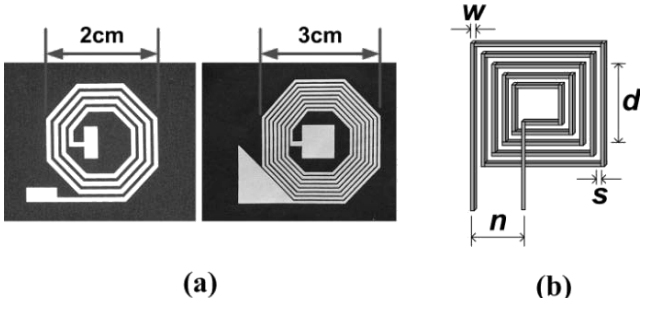

Fig. 2 (a) Wearable inductor photo, (b) Design parameters.

In addition, the inductance value can be changed dynamically during operation. It is because the human body is always moving to warp the fabric changing the effective diameter from the initial state. For instance, wearable inductor can be attached on the chest or wrist for ECG monitoring [3] and blood pressure monitoring [9], respectively. Since the wrist or chest is cylinder-shaped, the inductance is changed from its original value. Moreover, fabric substrates of the wearable inductor are deformed by the user's movement such as waving, stretching, lowering, or raising his/her arm [13]. To verify the effect of this deformation, 61 wearable inductors are manufactured and attached to the wrist or chest of different 5 persons taking several poses with their body; resulting in 222 times of measurements in total. As a result, this kind of dynamic variation is measured as the maximum 31.86% additional variances from the initial value as shown in Fig. 1.

17% static and 31.86% dynamic variations of inductance value can make inductive coupling communication very unreliable. Even though different signaling methods, narrow-band and wide-band signaling [14], are used, the static and dynamic variations affects both of them regardless of the signaling methods. The detailed comparison between two signaling methods in terms of the reliability and efficiency of the communication will be discussed in next section.

2.2 Wearable Inductor Channel

A pair of wearable inductors forms a wearable inductor channel for data communication. There are two signaling methods, narrow-band and wide-band signaling. Narrow-band signaling uses a carrier modulation with a single tone frequency carrier, and wide-band signaling uses wide band frequency signal like the pulse signal. The channel gain (A), the ratio of the transmitted voltage amplitude to the received voltage amplitude, is examined by varying the inductance value of the receiver to evaluate the channel properties. It is very effective because all parameters such as misalignment, distance, and the relative angle between two inductors of the channel affect the gain [9]. Since the more effective channel has the larger gain, narrow-band signaling is more effective than wide-band signaling when the resonance frequency of the transmitter and receiver inductor is near.

However, narrow-band signaling is very susceptible to the inductance variation compared to the wide-band signaling. For reliable communication, the inductance variation should be compensated for the gain to be stable. But there was no report on the resonance compensation technique for

the narrow band signaling, and only for wide-band signaling inductive communication was reported without the real-time compensation [5]. In this work, for the first time, real-time capacitor compensation technique is proposed for the narrow-band signaling.

3. Transceiver Design

Figure 3 shows the top architecture of the proposed inductive coupling transceiver. It is composed of the Pulsed-Clock On-Off Keying (PC-OOK) transceiver for reducing power consumption, RLC Bridge, Real-time Capacitor Compensation (RCC) block for detection and compensation of the inductance variation during data transmission, and Clock Data Recovery (CDR) circuit which is designed as [15]. The RLC Bridge is shared between PC-OOK receiver and RCC block.

3.1 PC-OOK Transmitter

The concept of PC-OOK modulation, a kind of modification from the conventional On-Off Keying (OOK) modulation, is shown in Fig. 4. To reduce power consumption, the PC-OOK transmitter shortens the carrier transmission time for data '1.' For example, the carrier transmission time is only 300 ns in the proposed PC-OOK modulation when the data rate is 250 kbps, while 4 μs is needed in the conventional OOK modulation. The relationship between input $x(t)$ and output signal $y(t)$ of PC-OOK transmitter is derived as in Eq. (2):

$$\begin{aligned} &y((\alpha-1)\cdot t' + t) \\ &\quad = f_c \cdot (x(\alpha-1)\cdot t' + t) - u_\alpha((\alpha-1)\cdot t' + t - \tau) \\ &\qquad (0 \le t \le t',\ \text{and } \alpha \text{ is the natural number}) \end{aligned} \tag{2}$$

while f_c is 13.56 MHz carrier signal, t' is a period at the corresponding data rate, α is the serial number of data sequence which starts from 1, and $x(t)$, $u_\alpha(t)$ and τ has the following constrains as in (3):

$$\begin{aligned} &x(t) = 0 \quad (t \le 0) \\ &u_\alpha(t) = \begin{cases} x(t) & ((\alpha-1)\cdot t' \le t \le \alpha \cdot t') \\ 0 & (\text{Otherwise}) \end{cases} \\ &\tau = \begin{cases} 300\,\text{ns} & (t' \ge 300\,\text{ns}) \\ t' & (t' < 300\,\text{ns}) \end{cases} \end{aligned} \tag{3}$$

When the period t' is less than 300 ns, PC-OOK modulation becomes the same as conventional OOK modulation. Otherwise, it reduces the transmission time to 300 ns in the case of data '1.' To express the non-return to zero (NRZ) form of input $x(t)$, $u_\alpha(t)$ is defined as a step function that has the value of '1' within the range of one period (t') only.

By using this proposed PC-OOK modulation scheme, power consumption of the transmitter can be reduced up to 3.6 μW, which is 13.4% reduction from the conventional one.

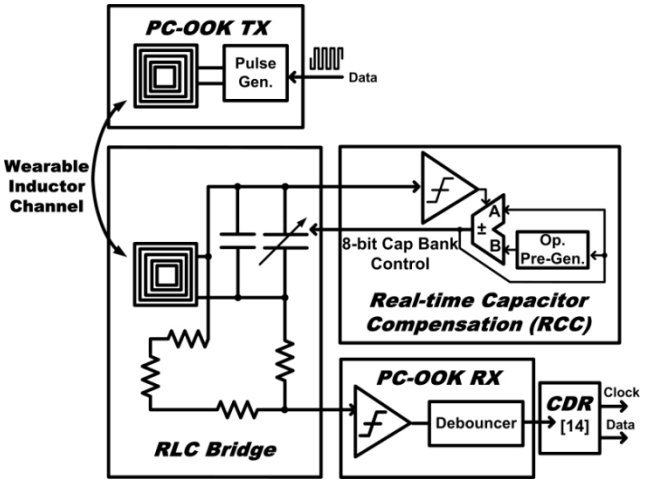

Fig. 3 Top architecture of the proposed transceiver.

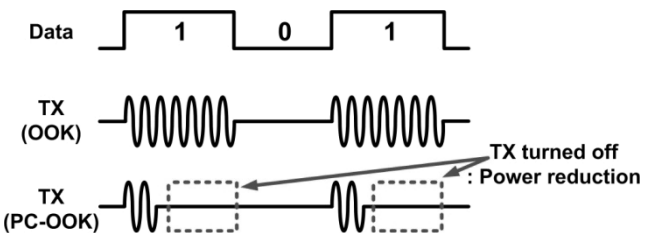

Fig. 4 Concept of PC-OOK.

3.2 PC-OOK Receiver

The PC-OOK receiver uses RLC Bridge and a threshold comparator to filter only the signal near the carrier frequency with high selectivity. Figure 5(a) shows the block diagram of the PC-OOK receiver. It consists of a threshold comparator and the RX debouncer. The voltage difference between the two reference voltages V_{REFP} and V_{REFN} of a threshold comparator can be adjusted according to the mutual inductance of each wearable inductor pair. In order to make the threshold comparator operate normally, we assume that V_{REFP} is always larger than V_{REFN}. The output signals of RLC Bridge named *INP* and *INN* in Fig. 6 are sent to the threshold comparator. And by using the magnitude difference between *INP* and *INN*, the received data is recovered in accordance with the relation in (4):

$$RXOUT = \begin{cases} 0 & (INN - INP \le V_{\mathrm{REFP}} - V_{\mathrm{REFN}}) \\ 1 & (INN - INP > V_{\mathrm{REFP}} - V_{\mathrm{REFN}}) \end{cases} \tag{4}$$

The RX debouncer circuit is added to hold the output for one clock period when the data is '1.' It is implemented by one D Flip Flop, and some logic gates. When there is the first transition from low to high in the input data, named *TCOUT*, of the RX debouncer, the D Flip Flop starts sampling *TCOUT* by delayed *TCOUT*. After the pre-determined time is passed from the last sampling of data '1,' reset signal of the D Flip Flop is enabled so that the output of the RX debouncer, named *RXOUT*, becomes low.

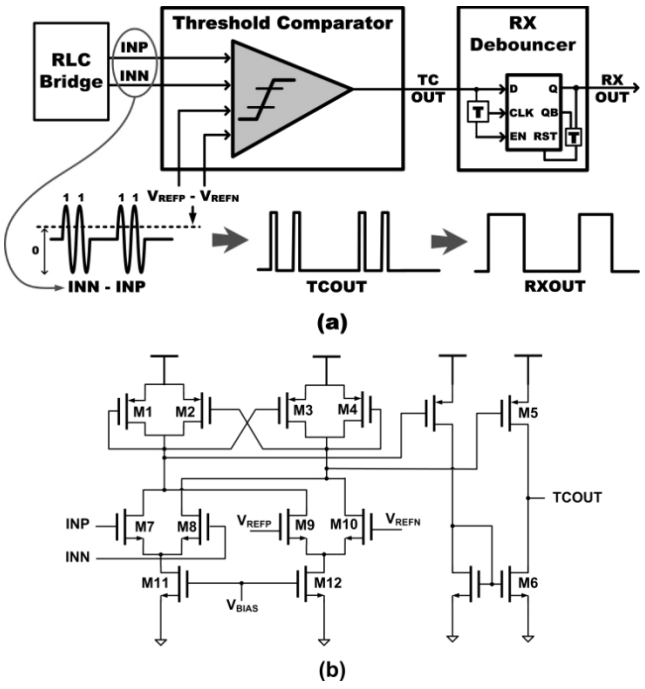

Fig. 5 PC-OOK Receiver. (a) Receiver block diagram, (b) Threshold comparator circuit.

The detailed circuit of a threshold comparator is shown in Fig. 5(b). The PMOS transistors M1 ∼ M4 make the circuit act as a comparator with hysteresis. It adopts the cross-coupled PMOS structure using M2 and M3, which enlarges the small difference between *INP*, *INN*, V_{REFP} and V_{REFN} using positive feedback so that the output of the threshold comparator is determined quickly. And the size of M1 and M4 is determined as the same as M2 and M3. M5 and M6 are used to make *TCOUT* have the full range from VDD to GND. The low threshold voltage NMOS transistors are used for M11 and M12 to achieve the wide input range. Its threshold voltage is 260 mV while 475 mV for basic NMOS transistor.

3.3 RLC Bridge

In Fig. 6, the RLC Bridge structure is shown. It includes the wearable inductor, 4 resistors, and 8-bit capacitor bank with one external capacitor connected in parallel. The value of resistance *R1* ∼ *R4*, inductance *L*, the total capacitance *C*, and resonance frequency of the parallel LC tank ω have the following relationship as in (5):

$$\omega^2 = \frac{1}{L \cdot C}$$
$$R1 \cdot R3 = R2 \cdot R4 \tag{5}$$

According to Eq. (5), all 4 resistors are 100 Ω, and they are implemented by on-chip resistors. And the 8-bit capacitor bank can be adjusted by Real-time Capacitor Compensation block. Its unit capacitance value is 500 fF, and the external capacitance is 32 pF. In the RLC Bridge of Fig. 6, the output

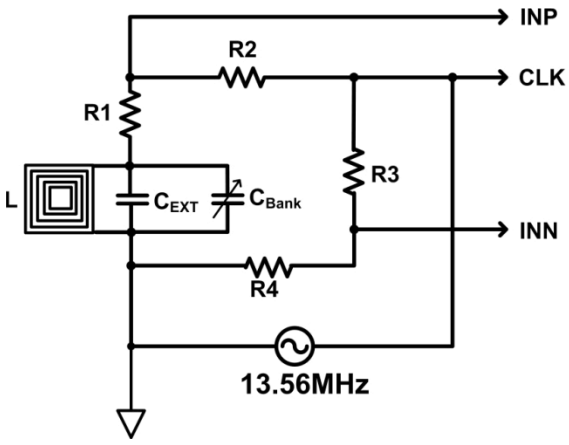

Fig. 6 RLC Bridge structure.

voltage magnitude $|INP - INN|$ is maximized when ω is exactly the same as the clock frequency so that the impedance of the parallel LC tank becomes infinity. And the larger the difference between resonance and clock frequency is, the smaller the output voltage magnitude is. Otherwise, if the LC tank is placed in series, the output voltage magnitude is minimized when the resonance frequency becomes the same as clock frequency [16]. So the capacitance value of the RLC Bridge should be properly set in order to classify the received data as '0' or '1' clearly even though the inductance value is varied. In the proposed transceiver, the total capacitance value is adjusted to tune its resonance frequency to the carrier frequency of the received signal of 13.56 MHz by Real-time Capacitor Compensation (RCC) block in Sect. 4.

4. Real-Time Capacitor Compensation (RCC)

Figure 7 shows the RCC block diagram consisting of RLC Bridge, the Dual-edge Sampling Comparator, the operand pre-generator, and the Adder/Subtractor. The RLC Bridge is shared with PC-OOK receiver as shown in Fig. 3. The Dual-edge Sampling Comparator determines whether the additional capacitors be added or subtracted to the current capacitance in order to tune the resonance frequency to 13.56 MHz. And the operand pre-generator achieves fast compensation by optimized algorithm for wearable inductance variations.

4.1 Real-Time Capacitor Compensation (RCC) Principle

To detect and compensate for the inductance variation in real-time, RLC Bridge in PC-OOK receiver is used in the RCC block at the same time. During data transmission, phase of the signal *INP*($\angle$INP), which is output of the RLC Bridge, is changed as in Eq. (6):

$$\angle \mathrm{INP} = \tan^{-1}\left(\frac{\sqrt{L \cdot (1 + \Delta L)/C_0}}{R \cdot \Delta L}\right) \tag{6}$$

where C_0 and L_0 are the original capacitance and inductance, respectively, and their resonance frequency is

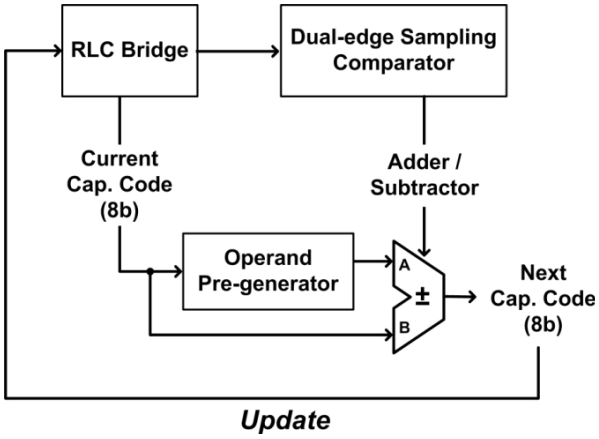

Fig. 7 RCC block diagram.

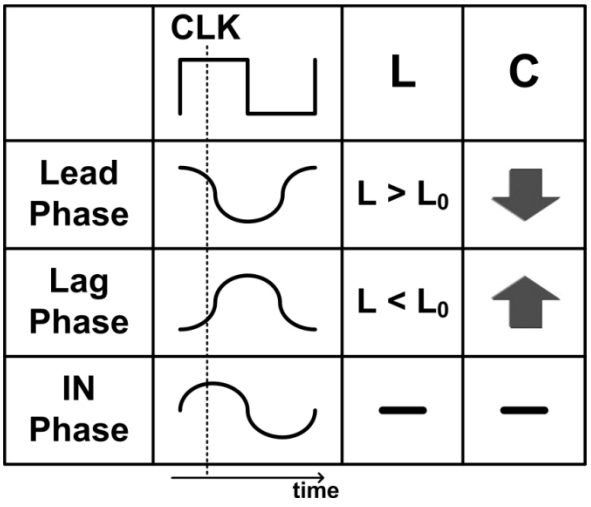

Fig. 8 Case summary of phase relationship between INP and CLK.

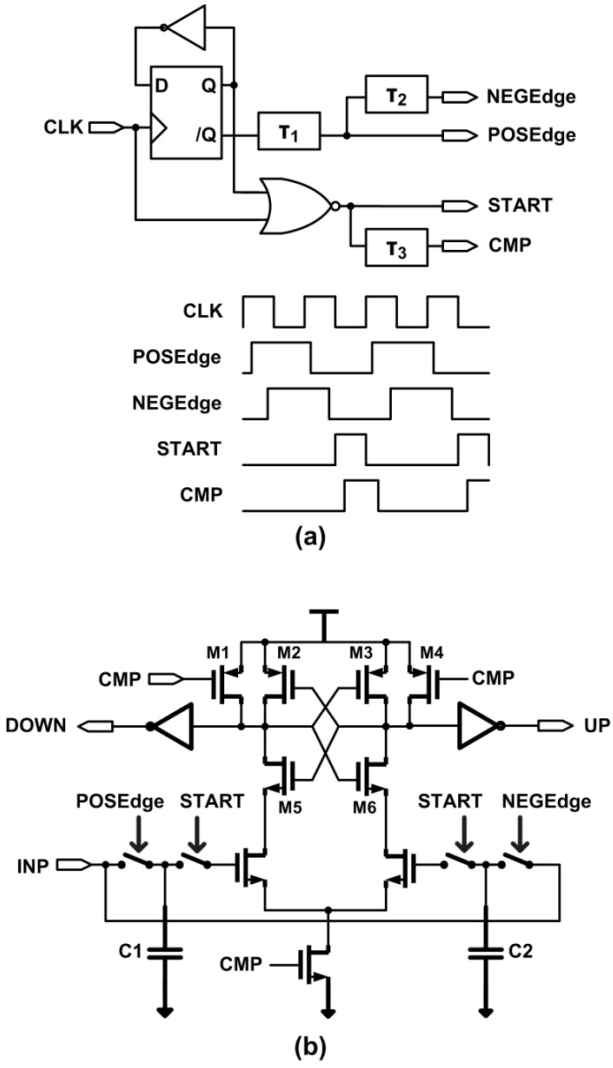

Fig. 9 Dual-edge sampling comparator. (a) Control signal timing diagram, (b) Circuit.

13.56 MHz. R is the resistor of RLC Bridge which is 100 ohm in this work. C and L are the capacitance and inductance values after the variation occurs, then L is given by L_0 and the amount of variation ΔL as Eq. (7):

$$L = L_0(1 + \Delta L) \tag{7}$$

There are three cases of phase relationships between INP and CLK as the inductance value varies. The time-domain waveform, inductance variation, and the direction of the capacitance change according to three cases are summarized in Fig. 8. For the first case, *Lead Phase*, the inductance variation is positive, ∠INP or be positive by Eq. (6) and the phase of INP leads that of *CLK*. And in this case, the capacitance value should be decreased in order to the resonance frequency remains the same. For the second case, *Lag Phase*, the capacitance value needs to be increased since the inductance is decreased causing that ∠INP becomes negative and lags the phase of *CLK*. Finally, in the third case, *IN Phase*, when the phase difference between *INP* and *CLK* is zero, the capacitance value should remain the same.

4.2 Dual-Edge Sampling Comparator

To determine the direction of capacitance change, Dual-edge Sampling Comparator compares the signal at positive *CLK* edge with the signal at negative *CLK* edge, and determines the phase of LC tank. Figure 9 shows the control signal timing diagram and the circuit of Dual-edge Sampling Comparator. There are 4 control signals, named *NEGEdge*, *POSEdge*, *START*, and *CMP*, in the Dual-edge Sampling Comparator, and all of them are generated from the signal *CLK* which is one of the outputs in RLC Bridge shown in Fig. 6. At the positive (negative) *CLK* edge, *POSEdge* (*NEGEdge*) switch is closed and *INP* signal is sampled into C1 (C2). Then sampled values in both capacitors are compared to each other at the next positive *CLK* edge. When the signal at positive edge is larger, *DOWN* will be high. If the signal at negative edge is larger, *UP* goes high and *DOWN* goes low. If the difference between two values is not big

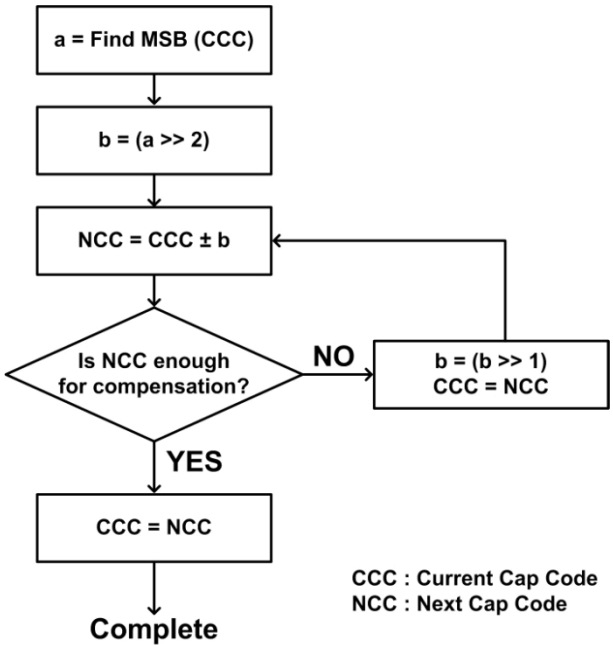

Fig. 10 State diagram of the proposed searching algorithm for capacitance compensation.

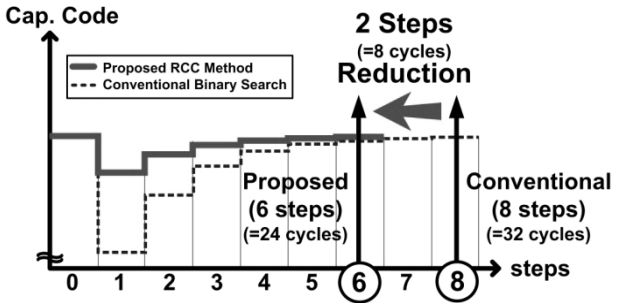

Fig. 11 Compensation time comparison between conventional and proposed searching method.

enough to complete comparison, both *UP* and *DOWN* stay low. *UP* and *DOWN* increases and decreases the capacitance value, respectively to determine whether Adder or Subtractor is selected for capacitance calculation as shown in Fig. 7.

C1 and C2 of Fig. 9(b) are implemented with NMOS capacitor. Since the *INP* signal go through the switch and capacitor, the RC time constant must be less than the highest frequency of *INP* which is 13.56 MHz in this work. Since on-resistance of the switch is 300 Ω, up to 39 pF of capacitance value can be adopted. With consideration of area consumption and speed, 1 pF of capacitance value is chosen for both C1 and C2. In the proposed Dual-edge Sampling Comparator, cross-coupled PMOS and NMOS structure with M2, M3, M5, and M6 is adopted. It acts as a sense-amp so that it enlarges the difference between two inputs. And M1 and M4 are used in order to make all outputs low when *CMP* is '0' so that it makes the Dual-edge Sampling Comparator prepare the next comparison.

4.3 Operand Pre-Generator

In order to find the proper capacitance value quickly for the compensation of the inductance variation, a fast searching algorithm, which is modified from the binary-weighted searching algorithm, is adopted in this work. Compared with simple binary-weighted search, the proposed algorithm reduces the size of a target set for searching. For example, if the current code is 1000_0000 with total 8-bit and the variance direction is increase, then the target set for next code has the range from 1000_0000 to 1011_1111 in proposed searching while from 1000_0000 to 1111_1111 in conventional one. So the target set size is reduced by half. Figure 10 shows the state diagram of this proposed searching algorithm for capacitance compensation. At the beginning, most significant bit (*a* in Fig. 10) of the 8-bit current capacitor code (*CCC* in Fig. 10) is found. Then *a* is 2-bit right shifted to get the first operand (*b* in Fig. 10) because the inductance variation does not exceed about ±30% during manufacturing process or operation as shown in Fig. 1. According to the Dual-edge Sampling Comparator, the next capacitor code (*NCC* in Fig. 10) is increased or decreased from *CCC* by *b*. If *NCC* is the right amount of capacitance for the compensation of inductance variation, the process is stopped and the capacitor code is updated. Otherwise, the process is repeated with the updated capacitor code, and the new operand of 1-bit right shift from the previous operand. Therefore, the proposed RCC scheme limits the capacitance selection range per one step up to 25% instead of 50% which was used in conventional binary-weighted searching algorithm.

The compensation time comparison between conventional and the proposed searching method is shown in Fig. 11. There are 4 clock cycles in each step of search. 2 cycles are to check the direction of compensation in Dual-edge Sampling Comparator, 1 cycle is to calculate *NCC* from *CCC* and *b* in operand pre-generator, and another 1 cycle is for changing capacitance according to the digital capacitor code. As a result, the proposed RCC scheme saves 2 steps, or 8 clock cycles for compensation in worst case. In other words, maximum 6 steps of searching can be processed, or the variation up to 49.2% (= 25% × (1 + 1/2 + 1/4 + 1/8 + 1/16 + 1/32)) of the original capacitor code can be covered. The RCC scheme begins the compensation process only 3 μs after the inductance variation occurs. In total, it takes 4.78 μs of compensation time including 3 μs of variance detection in worst case.

5. Implementation Results

The proposed inductive coupling transceiver is fabricated in 0.18 μm CMOS technology and the chip microphotograph is shown in Fig. 12. The total chip area including pads is 2.7 × 1.0 mm^2. RLC Bridge is shared between PC-OOK receiver and the RCC scheme, so two blocks are placed closely to each other in layout. All circuit measurements

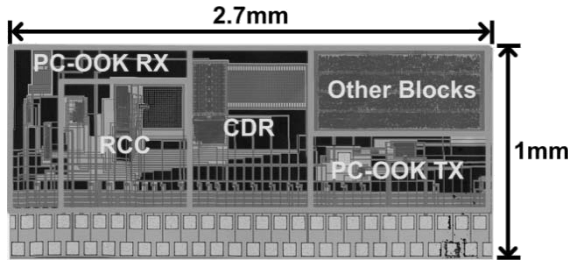

Fig. 12 Chip microphotograph.

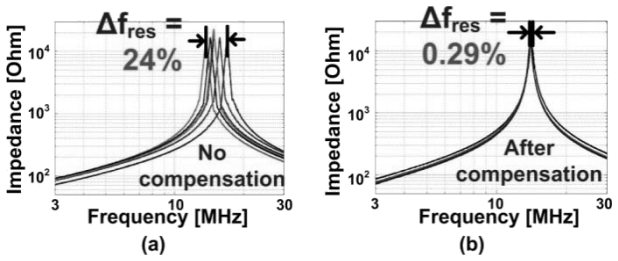

Fig. 13 Capacitor compensation results. (a) Without compensation, (b) With compensation.

are performed with a 1.8 V power supply.

Figure 13 shows the capacitor compensation results on the dynamic variance of planar wearable inductor. Figure 13(a) shows that the resonance frequency variation is 24% without compensation while the transceiver is worn, and Fig. 13(b) shows that the resonance frequency variation is reduced below to 0.29% with the proposed compensation scheme. Without capacitor compensation, SNR degradation amounts to 16.7 dB compared to the fixed capacitance value case. In contrast, by using the proposed RCC scheme, 13.36 dB of SNR enhancement can be achieved.

BER characteristics of the proposed transceiver according to the distance, misalignment, and the relative angle are measured as Fig. 14. The distance is a vertical distance between two inductors, and the misalignment is a horizontal distance between the centers of two inductors. And the relative angle is defined as the angle between the edges of two inductors as shown in Fig. 14(a). Since not the absolute amount of misalignment but the ratio between misalignment and inductor size affects the BER characteristics, the channel inductor is chosen to be big enough so that misalignment due to user's movement do not degrade the communication reliability. Figure 14(b) shows the measured BER characteristics. To achieve BER below to 10^{-3}, less than 3 cm of communication distance, 1 cm of misalignment, and 45° of relative angle is needed when two $1 \times 1\,\mathrm{cm}^2$ rectangular-shaped wearable inductor are used for communication. Transient measurement waveforms are also shown in Fig. 14(c). When BER is less than 10^{-3}, the transmission is successful as in the left figure of Fig. 14(c). However in the case that BER is higher than 10^{-3}, the data transmission is failed as in the right figure of Fig. 14(c).

Table 1 summarizes the performance of the proposed inductive coupling transceiver chip. The transceiver block

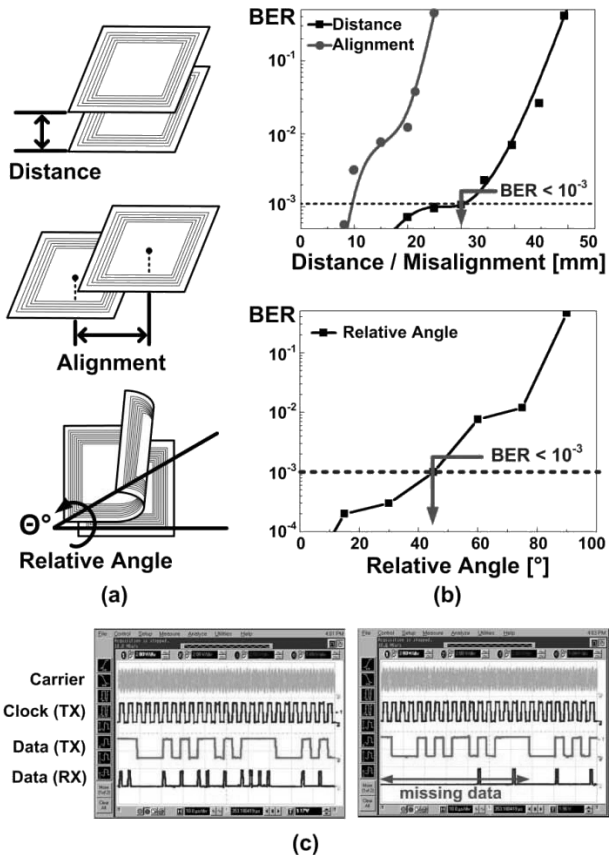

Fig. 14 BER characteristics. (a) Parameter description, (b) BER measurement at 4 Mbps data rate, (c) Transient waveform (Measurement).

Table 1 Performance summary.

Process	0.18μm CMOS technology	
Supply Voltage	Core	1.8V
	I/O	3.3V
Data Rate	Up to 4Mbps (Variable)	
Power Consumption (at 4Mbps)	TRX	32.4μW
	RCC	70.2μW
	CDR	324μW
BER < 10^{-3}	Distance	3cm
	Misalignment	1cm
	Relative angle	45°
Die Area	2.7mm x 1mm (including pads)	

consumes 32.4 μW and RCC scheme consumes 70.2 μW. All measurements are performed with two rectangular-shaped wearable inductors of 1 cm × 1 cm size. The performance comparison with the previous works is summarized in Table 2. Although some additional previous works also reported the automatic impedance matching technique [18]–[20] which is similar to inductance compensation technique in [5], all of them are not support the real-time compensation as this work. The proposed inductive coupling transceiver

Table 2 Performance comparison.

Performance Parameters	[5]	[17]	This Work
Supply Voltage	2.5V	1V	1.8V
Power Consumption (TRX + Compensation)	210μW	187μW	103μW
Compensation Type / # of steps in worst case	Periodically Check (Static) / 10 steps	Not Supported	Real-time (Dynamic) / 6 steps
Application	WBSN	Cm-range Wireless	WBSN

chip consumes the lowest power even with the real-time dynamic compensation circuits. It also shows the fastest compensation time with real-time variance detection.

6. Conclusion

This work presents an inductive coupling transceiver that can compensate for the dynamic inductance variation with capacitor compensation scheme in real-time for wearable body sensor network. For high efficiency of data communication, PC-OOK modulation with narrow-band signaling is adopted. Hence, 13.4% of power reduction compared to the conventional OOK modulation is achieved with comparable or longer communication distance in the transmitter. Also, in order to support the real-time detection and compensation for inductance variation, RCC scheme is proposed which shares RLC Bridge with PC-OOK receiver. Total compensation time takes only 4.78 μs in worst case, including 3 μs of variance detection. The transceiver is implemented with 0.18 μm CMOS technology and consumes 102.6 μW during operation.

References

[1] A. Lymberis and D. DeRossi, Wearable eHealth Systems for Personalised Health Management, IOS Press, Amsterdam, The Netherlands, 2004.
[2] H. Kim, Y. Kim, Y.-S. Kwon, and H.-J. Yoo, "A 1.12 mW continuous healthcare monitor chip integrated on a planar fashionable circuit board," ISSCC Digest of Technical Papers, pp.105–603, Feb. 2008.
[3] J. Yoo, L. Yan, S. Lee, Y. Kim, and H.-J. Yoo, "A 5.2 mW self-configured wearable body sensor network controller and a 12 μW wirelessly powered sensor for a continuous health monitoring system," IEEE J. Solid-State Circuits, vol.45, no.1, pp.178–188, Jan. 2010.
[4] A.C.-W. Wong, D. McDonagh, G. Kathiresan, O.C. Omeni, O. El-Jamaly, T.C.-K. Chan, P. Paddan, and A.J. Burdett, "A 1 V, micropower system-on-chip for vital-sign monitoring in wireless body sensor networks," ISSCC Digest of Technical Papers, pp.138–602, Feb. 2008.
[5] J. Yoo, S. Lee, and H.-J. Yoo, "A 1.12 pJ/b inductive transceiver with a fault-tolerant network switch for multi-layer wearable body area network applications," IEEE J. Solid-State Circuits, vol.44, no.11, pp.2999–3010, Nov. 2009.
[6] S. Lee, J. Yoo, H. Kim, and H.-J. Yoo, "A dynamic real-time capacitor compensated inductive coupling transceiver for wearable body sensor networks," 2009 Symposium on VLSI Circuits Digest of Technical Papers, pp.42–43, June 2009.
[7] R.N. Simons, F.A. Miranda, and J.D. Wilson, "Wearable wireless telemetry system for implantable bio-MEMS sensors," Proc. 28th Annual International Conference of the IEEE Engineering in Medicine and Biology Society (EMBC), 2006.
[8] S. Lee, J. Yoo, and H.-J. Yoo, "A healthcare monitoring system with wireless woven inductor channel for body sensor network," Proc. 5th International Workshop on Wearable and Implantable Body Sensor Networks (BSN), pp.62–65, 2008.
[9] S. Lee, J. Yoo, and H.-J. Yoo, "A wearable inductor channel design for blood pressure monitoring system in daily life," 3rd International Conference on Pervasive Computing Technologies for Healthcare, April 2009.
[10] Y. Kim, H. Kim, and H.-J. Yoo, "Electrical characterization of printed circuit on the fabric," IEEE Trans. Adv. Packag., vol.33, no.1, pp.196–205, Feb. 2010.
[11] S. Lee, B. Kim, and H.-J. Yoo, "Planar fashionable circuit board technology and its applications," J. Semiconductor Technology and Science, vol.9, no.3, pp.174–180, Sept. 2009.
[12] S. Lee, J. Yoo, K. Song, and H.-J. Yoo, "A 1.13 pJ/b inductive coupling transceiver with adaptive gain control for Cm-range 50 Mbps data communication," IEEE Asian Solid-State Circuit Conferences, pp.297–300, Nov. 2009.
[13] S.W. Oh, J. Noh, and K. Wohn, "A physically faithful multigrid method for fast cloth simulation," J. Computer Animation and Virtual World, vol.19, no.3-4, pp.479–492, Sept. 2008.
[14] N. Miura, D. Mizoguchi, T. Sakurai, and T. Kuroda, "Analysis and design of inductive coupling and transceiver circuit for inductive inter-chip wireless superconnect," IEEE J. Solid-State Circuits, vol.40, no.4, pp.829–837, April 2005.
[15] S.-J. Song, N. Cho, and H.-J. Yoo, "A 0.2-mW 2-Mb/s digital transceiver based on wideband signaling for human body communications," IEEE J. Solid-State Circuits, vol.42, no.9, pp.2021–2033, Sept. 2007.
[16] J.G. Webster, ed., The measurement, instrumentation, and sensors handbook, chap.50, CRC Press LLC, 1999.
[17] D. Guermandi, S. Gambini, and J. Rabaey, "A 1 V 250 kpps 90 nm CMOS pulse based transceiver for cm-range wireless communication," Proc. IEEE European Solid-State Circuits Conference, pp.135–138, Sept. 2007.
[18] A.R.A. Keane and S.E. Hauer, "Automatic impedance matching apparatus and method," U.S. Patent, no.5195045, 1993.
[19] A. Chamseddine, J.W. Haslett, and M. Okoniewski, "CMOS silicon-on-sapphire RF tunable matching networks," EURASIP J. Wireless Communications and Networking, vol.2006, pp.1–11, 2006.
[20] D. Qiao, D. Choi, Y. Zhao, D. Kelly, T. Hung, D. Kimball, M. Li, and P. Asbeck, "Antenna impedance mismatch measurement and correction for adaptive CDMA transceivers," IEEE MTT-S International Microwave Symposium, June 2005.

Seulki Lee received the B.S. and M.S. degrees from Korea Advanced Institute of Science and Technology (KAIST), Daejeon, in 2007 and 2009, respectively, where she is currently working toward the Ph.D. degree, all in electrical engineering. Her current research interests include the inductive coupling transceiver design and near-field communication for wearable applications.

Jerald Yoo received the B.S., M.S., and Ph.D. degrees in Department of Electrical Engineering from the Korea Advanced Institute of Science and Technology (KAIST), Daejeon, Korea, in 2002, 2007, and 2010, respectively. In May 2010, he joined the faculty of Microsystems Engineering, Masdar Institute, Abu Dhabi, United Arab Emirates, where he is an assistant professor. He is currently also with Microsystems Technology Laboratory, Massachusetts Institute of Technology (MIT), Cambridge, MA, USA, as a visiting scholar. As a chief researcher at the Semiconductor System Laboratory in KAIST, he developed low-energy Body Area Network (BAN) transceivers and wearable body sensor network using Planar-Fashionable Circuit Board (P-FCB) for continuous health monitoring system. His research focuses on low energy circuit technology for wearable bio signal sensors, wireless power transmission, SoC design to system realization for wearable healthcare applications, and energy-efficient biomedical circuit techniques. He is an author of the book chapter in Biomedical CMOS ICs (Springer, 2010). Dr. Yoo is a co-recipient of the Asian Solid-State Circuits Conference (A-SSCC) Outstanding Design Awards in 2005.

Hoi-Jun Yoo graduated from the Electronic Department of Seoul National University, Seoul, Korea, in 1983 and received the M.S. and Ph.D. degrees in Department of Electrical Engineering from the Korea Advanced Institute of Science and Technology (KAIST), Daejeon, in 1985 and 1988, respectively. His Ph.D. work concerned the fabrication process for GaAs vertical optoelectronic integrated circuits. From 1988 to 1990, he was with Bell Communication Research, Red Bank, NJ, where he invented the two-dimensional phase-locked VCSEL array, the front-surface-emitting laser, and the high-speed lateral HBT. In 1991, he became a manager of the DRAM design group at Hyundai Electronics and designed a family of fast-1M DRAMs to 256M synchronous DRAMs. In 1998, he joined the faculty of the Department of Electrical Engineering at KAIST and now is a full professor. From 2001 to 2005, he was the director of System Integration and IP Authoring Research Center (SIPAC), funded by Korean Government to promote worldwide IP authoring and its SoC application. From 2003 to 2005, he was the full time Advisor to Minister of Korea Ministry of Information and Communication and National Project Manager for SoC and Computer. In 2007, he founded System Design Innovation & Application Research Center (SDIA) at KAIST to research and to develop SoCs for intelligent robots, wearable computers and bio systems. His current interests are high-speed and low-power Network on Chips, 3-D graphics, Body Area Networks, biomedical devices and circuits, and memory circuits and systems. He is the author of the books *DRAM Design* (Seoul, Korea: Hongleung, 1996; in Korean), *High Performance DRAM* (Seoul, Korea, Sigma, 1999; in Korean), *Low-Power NoC for High-Performance SoC Design* (CRC Press, 2008), and chapters of *Networks on Chips* (New York, Morgan Kaufmann, 2006). Dr. Yoo received the Electronic Industrial Association of Korea Award for his contribution to DRAM technology in 1994, the Hynix Development Award in 1995, the Design Award of ASP-DAC in 2001, the Korea Semiconductor Industry Association Award in 2002, the KAIST Best Research Award in 2007, the Asian Solid-State Circuits Conference (A-SSCC) Outstanding Design Awards in 2005, 2006, and 2007, and the DAC/ISSCC Student Design Contests Award in 2007 and 2008. He is an IEEE fellow and serving as an Executive Committee Member and the Far East Secretary for IEEE ISSCC, and a Steering Committee Member of IEEE A-SSCC. He was the Technical Program Committee Chair of A-SSCC 2008.